RMetS
Royal Meteorological Society

Modelling sea-breeze climatologies and interactions on coasts in the southern North Sea: implications for offshore wind energy

C. J. Steele,[a]* S. R. Dorling,[a,b] R. von Glasow[a] and J. Bacon[b]
[a]*School of Environmental Sciences, University of East Anglia, Norwich, UK*
[b]*Weatherquest Ltd., School of Environmental Sciences, University of East Anglia, Norwich, UK*

*Correspondence to: C. J. Steele, Centre for Ocean and Atmospheric Sciences, School of Environmental Sciences, University of East Anglia, Norwich NR4 7TJ, Norfolk, UK. E-mail: christopher.steele@uea.ac.uk

Current understanding of the behaviour of sea breezes in the offshore environment is limited but rapidly requires improvement due, not least, to the expansion of the offshore wind energy industry. Here we report on contrasting characteristics of three sea-breeze types on five coastlines around the southern North Sea from an 11 year model-simulated climatology. We present and test an identification method which distinguishes sea-breeze types which can, in principle, be adapted for other coastlines around the world. The coherence of the composite results for each type demonstrates that the method is very effective in resolving and distinguishing characteristics and features. Some features, such as jets and calm zones, are shown to influence offshore wind farm development areas, including the sites of the proposed wind farms up to 200 km offshore. A large variability in sea-breeze frequency between neighbouring coastlines of up to a factor of 3 is revealed. Additionally, there is a strong association between sea-breeze type on one coastline and that which may form coincidentally on another nearby. This association can be as high as 86% between, for example, the North Norfolk and East Norfolk coasts. We show, through associations between sea-breeze events on coastlines with contrasting orientations, that each coastline can be important for influencing the wind climate of another. Furthermore, we highlight that each sea-breeze type needs separate consideration in wind power resource assessment and that future larger turbines will be more sensitive to sea-breeze impacts.

Key Words: sea breeze types; WRF; offshore wind energy; marine weather forecasting; southern North Sea; coastal jets

Received 26 July 2013; Revised 13 October 2014; Accepted 17 October 2014; Published online in Wiley Online Library 05 December 2014

1. Introduction

The sea breeze is defined as a circulation which is induced by a thermal contrast, between the land and sea, that overcomes the strength of the background or gradient wind (Atkinson, 1981; Simpson, 1994). Sea breezes can occur on any coastline with a sufficient thermal contrast and so it is not surprising that to date there are over 1300 articles on the subject. The structure and physics of the sea breeze are consequently well documented and thorough reviews can be found in Abbs and Physick (1992), Miller *et al.* (2003) and Crosman and Horel (2010).

Sea breezes are known to influence coastal air pollution (e.g. Pielke, 1991; Yerramilli *et al.*, 2009), the impact of heat-waves on public health (e.g. Simpson, 1994) and even severe flooding events (e.g. Golding *et al.*, 2005), creating a strong motivation to study sea breezes in the onshore environment. However, little attention has been paid to the characteristics of different sea-breeze types, which were first described by the sailing community (Houghton, 1984; Brettle and Smith, 1999) and subsequently by Miller *et al.* (2003), nor to the sea breeze in the offshore environment.

The classical representation of a sea breeze is one forming against an offshore gradient wind. During offshore gradient wind conditions, the sea breeze is identified from a reversal in the surface winds, and many existing identification methods rely on this for event diagnosis (e.g. Borne *et al.*, 1998; Azorin-Molina *et al.*, 2011b). Miller *et al.* (2003) describe the cases where the sea breeze forms in opposition to the gradient wind as *pure* sea breezes (Figure 1(a)). If there is an along-shore component to the gradient wind with the land surface to the left in the Northern Hemisphere, then the resulting surface divergence created at the coast, due to friction, strengthens the sea breeze and the circulation forms an elongated helix shape (Miller *et al.*, 2003). Such a circulation is

© 2014 The Authors. *Quarterly Journal of the Royal Meteorological Society* published by John Wiley & Sons Ltd on behalf of the Royal Meteorological Society.
This is an open access article under the terms of the Creative Commons Attribution License, which permits use, distribution and reproduction in any medium, provided the original work is properly cited.

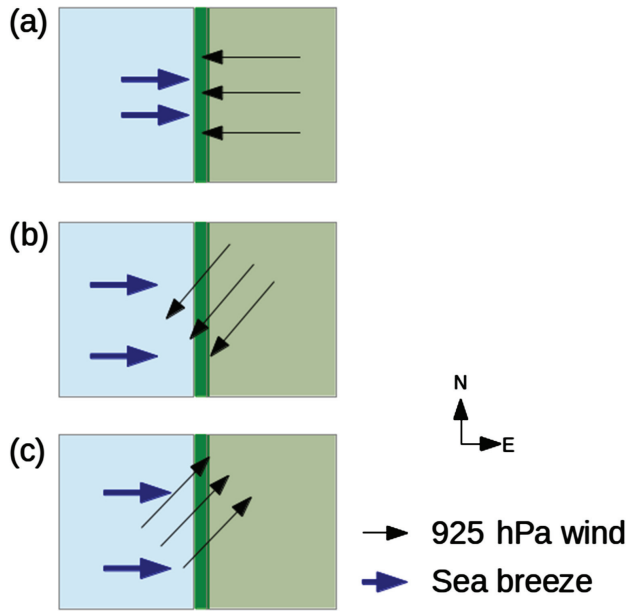

Figure 1. Schematics of the three sea breeze types with their associated gradient wind directions: (a) *pure*, (b) *corkscrew*, and (c) *backdoor*.

termed a *corkscrew* sea breeze (Figure 1(b)). In the opposite case, where there is an along-shore component to the gradient wind with the land surface to the right, a region of surface convergence is generated at the coast which weakens the circulation, forming a *backdoor* sea breeze (Figure 1(c)).

Early numerical studies on sea breezes, or those which focussed on equatorial cases, suggested that there were no differences between shore-parallel gradient winds representative of *corkscrew* or *backdoor* sea-breeze types (Arritt, 1993). However, in our earlier work (Steele *et al.*, 2013), we found that in such cases where Coriolis acceleration was non-zero, the shore-parallel component generated by Coriolis acceleration allowed the subsequent formation of the divergence or convergence responsible for distinguishing the *corkscrew* and *backdoor* types. Other studies, such as those by Gahmberg *et al.* (2010), identified the significance of the different sea-breeze types more implicitly by incrementally varying gradient wind speed and direction. These authors found a maximum in the strength of the sea breeze when the gradient wind direction was from a sector with a significant shore-parallel component with the land surface to the left. This is indicative of the stronger *corkscrew* type sea breeze, although this was not explicitly stated.

Offshore sea-breeze studies are often restricted to numerical simulations as measurement data in this environment are relatively scarce (e.g. Finkele, 1998; Gahmberg *et al.*, 2010; Steele *et al.*, 2013). Furthermore, the spatial scales of the sea breeze in the offshore environment are more difficult to distinguish, unlike the sea breeze in the onshore environment where the frontal boundary is usually well defined (Simpson, 1994). Arritt (1989) used a minimum landward wind speed threshold of $1\,\mathrm{m\,s^{-1}}$ to define the offshore bounds of the sea breeze. Offshore extents in the order of 100 km were simulated by both Arritt (1989) and Finkele (1998), however Finkele (1998) noted a greater degree of sensitivity of the offshore sea-breeze extent to gradient wind speed. Similarly, Steele *et al.* (2013) suggested that the sea-breeze offshore extent is sensitive to the chosen landward wind speed threshold, such that an increase to $1.5\,\mathrm{m\,s^{-1}}$ reduced the offshore spatial extent of the sea breeze by a third.

Our previous idealized numerical simulations (Steele *et al.*, 2013) showed that the offshore extent of the sea breeze is sensitive to the choice of planetary boundary-layer (PBL) scheme, particularly when the simulations include the addition of a second opposing coastline. The combination of a lack of measurements and a high degree of sensitivity to model set-up presents a challenge to those who utilize the offshore environment, including the sailing and offshore energy communities, as well as to weather forecasters.

In recent years, an unprecedented drive to construct a large number of offshore wind farms in the southern North Sea has begun (RenewableUK, 2014). Principally, this programme is driven by a desire to reduce global carbon emissions and to meet governmental renewable energy targets (EC, 2009). At the time of writing, the UK has 24 operational offshore farms amounting to 4.09 GW of installed capacity. By 2020, a further 15 larger farms will be constructed representing over 30 GW of additional capacity (RenewableUK, 2014). The sea breeze is an important component of the coastal and offshore wind climate and so will naturally have a role in resource assessment during the initial pre-construction phase of a wind farm. Furthermore, turbine power output is proportional to the cube of hub-height wind speed, so errors in wind speed forecasting are amplified in wind power forecasts. Such errors are not only costly in terms of ensuring adequate energy supplies to the customer, but over- or underestimations of power production can also have a substantial associated monetary cost. Since electricity production is contracted for 24 h ahead, underestimations of wind energy generation lead to a failure to realise revenue stream potential whilst overestimations attract a financial penalty, which requires the generator to make up the shortfall at the spot market price.

Therefore there is a strong motivation to fully understand the offshore wind climate. Since there is no existing method to identify all types of sea breeze, we present one which can be easily adapted for any coastline (section 2). The method is tested on five different coastlines around the southern North Sea using data from the Weather Research and Forecasting (WRF, version 3.3.1*; Skamarock and Klemp, 2008) model simulations spanning the period 2002–2012. Since there is a sensitivity to choice of PBL schemes, we also conduct some additional verification in section 3 using onshore and offshore observations. The results of the verification in section 3 inform the choice of gradient wind limits for the creation of the sea-breeze climatologies presented in section 4. In section 5 we attempt to quantify the spatial and temporal contributions of the sea breeze to wind energy for each sea-breeze type using a variety of simple methods based on the climatology results. Finally in section 6, the results are summarized and the implications are highlighted for the wind energy, sailing and weather forecasting stakeholder communities.

2. The sea-breeze identification method

It would be extremely laborious to subjectively identify sea breezes over an extended period. Therefore automated sea-breeze identification methods have been developed in order to determine whether specific criteria, or forecasting rules, are met. If all of the criteria are satisfied, then it is assumed that a sea breeze forms on that particular day. Existing sea-breeze identification methods include satellite-based, sea-breeze index and filter approaches. All methods either directly or indirectly determine the likelihood of a sea-breeze event by examining one or both of the large-scale windfield and the local thermal difference between land and sea.

A sea-breeze index typically compares these two components in the form of a ratio, where a critical ratio value dictates the likelihood of a sea breeze. The way in which either the background wind or the land–sea temperature contrast is calculated varies between indices. For example, Biggs and Graves (1962) used the ratio of offshore surface wind and the difference between the air temperature over the land and the water surface temperature. Lyons (1972) used the geostrophic wind speed at 1200 UTC instead of the surface observations used in Biggs and Graves (1962) to formulate the index. Both of these indices are very effective in forecasting sea-breeze days, however they exclusively focus on the

*Further discussion on the choice of model version can be found in section 4.

© 2014 The Authors. *Quarterly Journal of the Royal Meteorological Society* published by John Wiley & Sons Ltd on behalf of the Royal Meteorological Society.

pure sea breeze and do not explicitly include either the *corkscrew* or the *backdoor* types. Furthermore, the critical thresholds on which the methods rely are site-dependent (Miller *et al.*, 2003).

Remote-sensing methods (e.g. Damato *et al.*, 2003) rely on the formation of a line of cumulus along the convergence zone at the sea-breeze front in order to identify sea breeze events, though since cumulus are not always formed in sea-breeze events this method, like the index approach, cannot be applied universally. Furthermore, the use of satellite approaches confines the study to the times where the satellite data are available, thus potentially missing sea-breeze days.

Filter methods use a variety of tests to determine the likelihood of sea breezes. These can either take the form of a multi-scalar approach in which each stage, or filter, is working at progressively finer scales, or they involve looking specifically at the diurnal cycle. For example, Fichet *et al.* (2010) adopted a multi-scalar approach for the construction of a sea-breeze climatology in the Caen region of France. The first filter involved using the Objective Grosswetterlagen classification method (James, 2007) to identify the presence of anticyclonic conditions. A regional filter was then used to determine the land–sea thermal contrast before an agglomerative hierarchical clustering technique was finally used on measurement data from a network of temporary weather stations. In contrast, the filter method of Furberg *et al.* (2002) for sea-breeze events in Sardinia focussed almost exclusively on observations of wind speed. Their first filter examined the winds up to 6 h preceding sunrise to ensure that they were in the offshore direction. Their second filter captured days in which there was a sustained period of onshore flow during daylight hours. The third filter excluded days which experienced onshore winds during nocturnal hours and the final filter examined the land–sea temperature contrast, ensuring that the land was warmer by at least 3 °C.

Filter methods can also be conservative, where the sea breeze is identified by strict criteria, such as the timing and duration of the onshore flow (e.g. Furberg *et al.*, 2002). Such methods produce climatologies where sea-breeze frequencies are underestimated, however there is little ambiguity in those days which are identified.

The use of a filter method allows for the systematic determination of days in which conditions favouring a sea breeze exist on a variety of different spatial scales. The filter method is also much more generic than the other techniques, encompassing a wide range of possible scenarios to identify days when sea-breeze formation is plausible rather than explicitly resolved. Therefore this is the preferred method adopted here, as each filter can be refined to varying sensitivity and the performance of each individual filter can be easily examined.

Our approach is to use a filter method that uses a combination of model simulations and analyses at different spatial scales (Figure 2). The dependence on a model, rather than on observations, allows for a more complete regional description of the coastal wind climate, unconstrained by spatial (*in situ*) and temporal (satellite) limitations associated with measurements. Since very little is known about the *corkscrew* and *backdoor* sea-breeze types, a conservative method such as that of Furberg *et al.* (2002) is not suitable. The method is designed so that it could be adapted for use with any coastline around the world. However, the threshold criteria, such as land–sea thermal contrast, are likely to be dependent on the region being considered.

Our Filter 1 operates at the synoptic scale. Similar to Fichet *et al.* (2010), an objective classification method is used to classify the flow regime on a particular day. Here we use the Jenkinson–Collison method which uses sea level pressure fields from 6 h National Centers for Environmental Prediction (NCEP) FNL (Final) Global Tropospheric Analysis fields (NCEP *et al.*, 2000) to categorize flow regimes into different Lamb weather types (Jenkinson and Collison, 1977; Jones *et al.*, 1993). These are:

- **Anticyclonic**: Pure (A), northerly (AN), northeasterly (ANE), easterly (AE), southeasterly (ASE), southerly (AS), southwesterly (ASW), westerly (AW) and northwesterly (ANW).
- **Cyclonic**: Pure (C), northerly (CN), northeasterly (CNE), easterly (CE), southeasterly (CSE), southerly (CS), southwesterly (CSW), westerly (CW) and northwesterly (CNW).
- **Pure directional**: Northerly (N), northeasterly (NE), easterly (E), southeasterly (SE), southerly (S), southwesterly (SW), westerly (W) and northwesterly (NW).

The weather type is determined from both calculations of the zonal and meridional components of the gradient wind speed and the degree and sign of the vorticity over a specified area. Further details of the methodology of the Lamb weather typing are provided in the supporting information, Appendix S1, Figure S1. The Lamb weather type method was first developed for the UK though it has also been used in European climate studies including application to sea-breeze identification in the Bay of Alicante, Spain (e.g. Azorin-Molina *et al.*, 2011a). The original classification uses 1200 UTC analyses to determine the weather type. Here, we use the 6 h Global Forecasting System (GFS) Final Analysis from 1 January 2002 to 31 December 2012. The first filter rejects days on which cyclonic weather types are present at 0600, 1200, or 1800 UTC which would either prevent the sea breeze from forming or would make it too difficult to determine sea-breeze type because of cyclonic rotation of the gradient wind.

Our Filter 2 tests whether the Lamb weather type flow direction changes by more than 90° in any one direction between any of the 0600, 1200 and 1800 UTC analyses. If this is the case then the day is rejected since identification of sea-breeze type would prove difficult due to rapidly changing gradient wind direction, although it is acknowledged that sea breezes can change type and take on new characteristics during the day (Miller *et al.*, 2003). This filter accounted for only 1% of rejected days during the entire analysis (Figure 2).

Filter 3 works on the regional scale using simulations from the WRF model. In our set-up, the model has three two-way interactively nested domains of 27, 9 and 3 km horizontal grid spacing respectively (Figure 3(a)). GFS Final Analyses are used for lateral boundary conditions and sea surface temperature (SST) is updated by daily NCEP real-time SST Analyses interpolated to every 6 h. Six hourly analysis nudging is enabled for each simulation. Model physics are given in Table 1. Preliminary tests were run between 1 May and 30 September 2006 to assess the model sensitivity to the choice of PBL scheme. The simulations were compared against observations at the Cabauw tower (51.97°N, 4.93°E; Figure 3(b)) and at the Egmond aan Zee offshore mast (52.6°N, 4.38°E; Figure 3(b)) to determine the most suitable choice of PBL scheme for the sea-breeze climatologies. The results of the verification are presented in section 3.

The purpose of Filter 3 is to calculate, from the WRF model simulations, the local 925 hPa wind strength and direction relative to the target coastline. This is used to determine both the sea-breeze type and to reject days in which the gradient wind strength is too strong. Sensitivity tests reported in Steele (2013) suggested that the use of higher-altitude levels for this calculation was detrimental to performance of the identification method. Steele *et al.* (2013) found, through idealized simulations, that the simulated maximum gradient wind speed threshold required to allow formation of *pure* and *backdoor* sea breezes is sensitive to the choice of PBL scheme. Filter 3 adopts these thresholds and rejects days in which the simulated 925 hPa gradient wind speed is too strong.

The final filter (Filter 4) examines the land–sea temperature contrast, using averaged maximum 2 m air temperature over user-specified areas over both land and sea (Appendix S1, Figure S2). Alternative combinations of 2 m temperature and surface skin temperature were tested for sensitivity to thermal contrast but the averaged diurnal cycles of model variables did not reveal a sea-breeze signature, such as the presence of a

© 2014 The Authors. *Quarterly Journal of the Royal Meteorological Society* published by John Wiley & Sons Ltd on behalf of the Royal Meteorological Society.

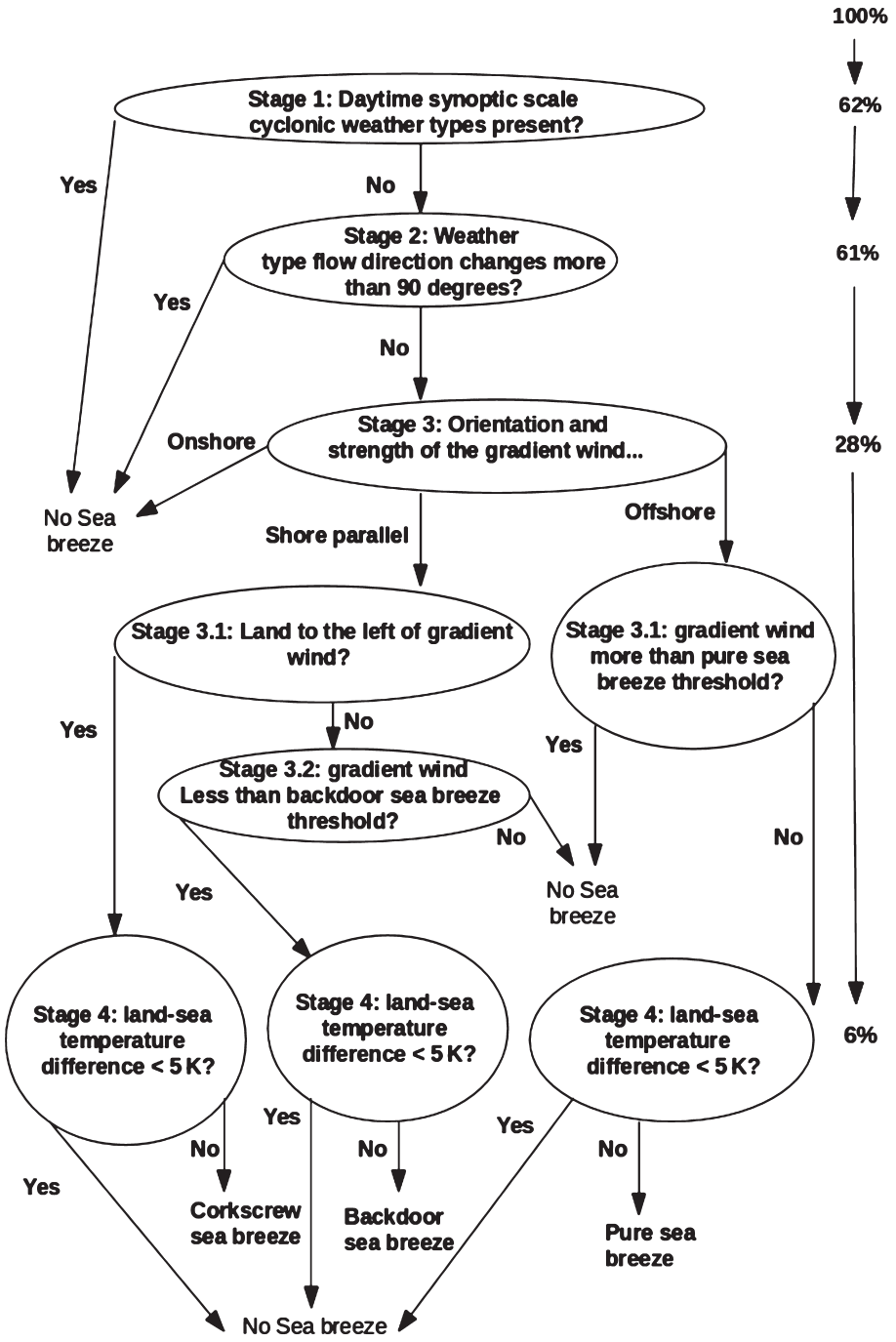

Figure 2. Flow chart of the filters involved in the sea-breeze identification method. The percentage of days passed by each filter for a typical coastline between 1 January 2002 and 31 December 2012 is shown on the right-hand side.

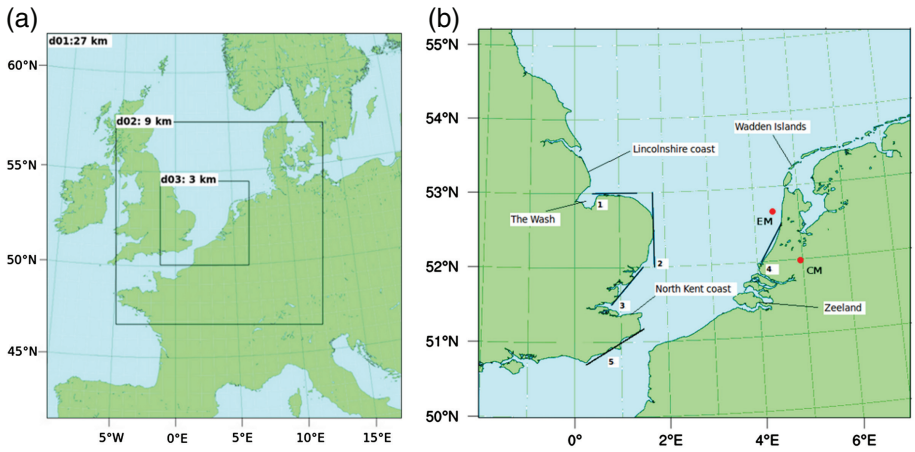

Figure 3. (a) WRF model domains as used in the construction of the sea-breeze climatologies. (b) Analysed coastlines using the filter-type identification method are labelled 1–5. These are: 1 North Norfolk; 2 East Norfolk; 3 Suffolk and Essex; 4 Netherlands; 5 South Kent. The positions of the masts are also shown (EM = Egmond aan Zee; CM = Cabauw).

© 2014 The Authors. *Quarterly Journal of the Royal Meteorological Society* published by John Wiley & Sons Ltd on behalf of the Royal Meteorological Society.

Table 1. WRF model and physics specifications used for the climatological simulations. The choice of PBL scheme was determined from verification against observations at onshore and offshore masts detailed in section 3. Note also that the cumulus scheme was applied only to d01.

WRF model settings	Details
Horizontal resolution (km)	d01: 27, d02: 9, d03: 3
Long-wave physics	RRTM
Short-wave physics	Dudhia shortwave
Model top (hPa)	50
Ground physics	Noah land surface
PBL scheme	YSU, MYJ, MYNN
Vertical levels	35; 8 in lowest 1 km
Cumulus scheme	Kain–Fritsch
Microphysics	WRF Single Moment 3 Class (WSM-3)
Surface physics	Monin-Obukhov

convergence line onshore. Therefore, it is likely that using area-averaged 2 m air temperature to calculate the land–sea thermal contrast does not pass as many non-sea breeze days as when using surface skin temperature, however the former case may also be too conservative. Additional information on the sensitivity tests performed are reported in Steele (2013). The minimum 2 m air temperature difference threshold required to pass this filter was set at 5 K, following Simpson (1994) for the south coast of England.

In all, five different coastlines were analysed (Figure 3(b)): 1 North Norfolk; 2 East Norfolk; 3 Suffolk and Essex; 4 Netherlands; 5 South Kent. Each coastline varies in complexity and coastal orientation, giving a thorough evaluation of the performance of the identification method.

The North Norfolk coast is oriented west–east and is comparatively straight. The main complexity of this coast is the presence of the Lincolnshire coastline to the northwest. East Norfolk is located adjacent to North Norfolk. It is oriented north–south and is also comparatively straight, however the northern and southern extremes of the East Norfolk coastline are both convex in shape. The presence of the Dutch coast 200 km to the east tests the validity of the idealized results of Steele (2013) concerning the interactions between sea breezes forming on facing coastlines.

The coast of Suffolk and Essex is much more complex than those for North and East Norfolk, containing many bays and headlands. This coast is oriented southwest to northeast and has the added complexity of the North Kent coast to the south protruding approximately 80 km offshore from the southern Essex coast. Furthermore, to the east across the North Sea is the southern part of the Dutch coastline approximately 200 km offshore.

The Dutch coast is concave and orientated southwest–northeast. At the northern and southern edges of the coastline lie the Wadden Islands and Zeeland, respectively. Zeeland is a large complex river delta which has multiple coastal orientations each with the potential to produce sea breezes.

Finally, the southern coast of Kent is adjacent to the narrowest water body of all the coastlines tested. Orientated southwest–northeast, it is relatively straight and at the narrowest point the English Channel is approximately 30 km wide, where the Strait of Dover is also known to form a coastal jet, adding further complexity to the region (Capon, 2003).

In the model output fields, each coastline is analysed using the filter-type sea-breeze identification method for the period 1 January 2002 to 31 December 2012. Composites of the model fields on days in which sea breezes have been identified are then examined to determine the typical sea-breeze evolution. In order to determine the spatial and temporal impact on wind power, a simple power curve is applied to the simulated wind speed values. Turbine capacity factor is also calculated, where capacity factor is the ratio of power production to the theoretical maximum power output for a given time period expressed as a percentage. Days which pass for sea-breeze events are compared to those which fail on account of an insufficient land–sea thermal contrast, to quantify the spatial impact of the sea breeze on wind energy. The average diurnal cycle of theoretical wind power output for wind farm locations is also analysed and compared against observations at the Egmond aan Zee wind farm (Figure 3(b)).

The purpose of a filter method is to identify favourable conditions for the potential formation of a sea breeze, rather than guaranteeing the occurrence of one. It is therefore possible that the method could falsely identify a sea breeze in this regard. However, in section 4 evidence is presented which increases confidence in the reliability of the method through the identification of characteristic sea-breeze features in composites of sea-breeze event sets.

3. WRF model evaluation

The Cabauw tower, which forms part of the Cabauw Experimental Site for Atmospheric Research (CESAR), has been in operation since 26 October 1972. Situated 50 km inland (Figure 3(b)), it consists of seven vertical measurement levels at 1.5, 10, 20, 40, 80, 140 and 200 m each recording observations of temperature, humidity, wind speed and wind direction. The surrounding terrain is relatively homogenous and flat and, despite the distance inland, sea breezes are known to reach the tower (Tijm *et al.*, 1999, and S. Tijm, personal communication). In the offshore environment, the Egmond aan Zee mast was erected in 2005 and dismantled in 2010 (Figure 3(b)). The purpose of the mast was to record observations before, during and after the construction of the Egmond aan Zee wind farm, 10–18 km offshore from the Dutch coast. It had three measurement heights at 21.6, 70 and 116 m located so that temperature, wind speed and wind direction could be sampled at heights within the rotor radius of the 36 3 MW wind turbines at the farm.

Few studies examine the performance of PBL schemes in both the onshore and offshore environment, though it has been noted by Cheng *et al.* (2012) and Steele *et al.* (2013) that alternative PBL schemes differ substantially in their simulations of sea breezes in both environments. For example, the simulated maximum onshore wind speed of a *pure* sea breeze was found by Steele *et al.* (2013) to vary by up to 55%. Three different PBL schemes are examined: the non-local Yonsei State University (YSU; Hong *et al.*, 2006) scheme, the level 2.5 local 1.5-order Turbulent Kinetic Energy (TKE) Mellor–Yamada–Janjic scheme (MYJ; Mellor and Yamada, 1982) and the level 2.5 Mellor–Yamada–Nakanishi–Niino (MYNN: Nakanishi, 2001) TKE scheme. These schemes were chosen as they are examples of both local and non-local schemes which vary in complexity and which have performed to varying degrees of accuracy for different applications (e.g. Sun and Ogura, 1980; Esau and Byrkjedal, 2007; Krogsaeter *et al.*, 2011).

May to September 2006 is chosen as the validation period as it was an exceptionally warm and anticyclonic year, theoretically supportive of the formation of sea breezes, although sustained warmth also increases SST and consequently raises the minimum land temperature required to initiate sea breezes.

3.1. Cabauw (onshore)

The average diurnal cycle of 2 m temperature at Cabauw (Figure 4) reveals that all PBL schemes underestimate temperature, especially during the nocturnal hours. The YSU scheme simulates 2 m temperature more accurately than the other schemes overall, although differences are smaller during daylight hours. In terms of use with the sea-breeze identification method, the smaller differences between PBL schemes in simulating daytime maximum temperature for a given day implies that filter 4 (Figure 2) of the method is not greatly sensitive to the choice of PBL scheme.

Table 2 shows the monthly model error statistics of temperature, wind speed and specific humidity, linearly interpolated between adjacent model levels and compared to

© 2014 The Authors. *Quarterly Journal of the Royal Meteorological Society* published by John Wiley & Sons Ltd on behalf of the Royal Meteorological Society.

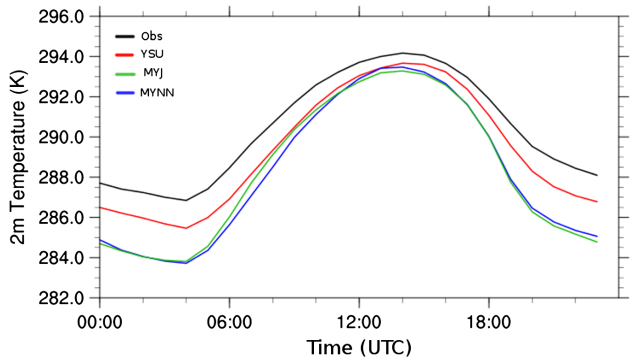

Figure 4. Observed and modelled average 2 m temperature diurnal cycle at Cabauw during May to September 2006. The nearest model gridpoint was 1.27 km northeast from the tower.

observations. The values shown are averaged over all heights of the Cabauw tower. Of the eight model levels below 1 km (Table 1), six are within the range 0–300 m (at approximately 10, 20, 40, 90, 180 and 300 m). The negative model bias associated with 2 m temperature (Figure 4) is a persistent feature across all levels and months and the improved performance of the YSU PBL scheme over the other two PBL schemes is again apparent.

However, the relative performance of each PBL scheme in simulating wind speed is less clear. The simulation of June using the YSU PBL scheme is the only one to give a slight negative model wind speed bias of $-0.01\,\mathrm{m\,s^{-1}}$. For all other months and PBL schemes, the bias errors are positive (Table 2). The MYNN PBL scheme has the largest error relative to the other schemes for wind speed during all months in terms of bias, mean absolute error (mae) and root mean square error (rmse). The scheme giving the best overall performance for wind speed is less clear. The mae for wind speed in June is slightly lower for the YSU scheme than for the MYJ (0.98 versus $1.02\,\mathrm{m\,s^{-1}}$). For all other months, the MYJ mae is either slightly lower or approximately equal to the YSU scheme. This pattern is also replicated using rmse as an error statistic. Similar to the temperature results, most of the error is generated when simulating the nocturnal PBL. During daylight hours, these differences between PBL schemes are substantially reduced.

Specific humidity is underestimated in all months using the YSU PBL scheme. The two TKE schemes overestimate the specific humidity during May, June and July. As with temperature, the scheme which produces the lowest errors in terms of mae and rmse at the Cabauw tower is the YSU. Unlike the other variables, there is no systematic error of specific humidity associated with time of day.

3.2. *Egmond aan Zee (offshore)*

The first point to note for the marine Egmond aan Zee mast is that the diurnal variability is much less than that over the land.

Table 2. Verification statistics (model minus observations) for WRF model simulations of temperature (temp), wind speed (Wspd) and specific humidity (Sp. hum) using three PBL schemes against measurements at the Cabauw tower and the Egmond aan Zee meteorological mast (here Wspd and Temp only as Sp. hum not recorded) during May to September 2006. WRF model data are first linearly interpolated to the observation heights before calculation of the error statistics. Values shown are averaged across all measurement levels for bias (BIAS), mean absolute error (MAE) and root mean square error (RMSE).

Measure	Month	BIAS			MAE			RMSE		
		YSU	MYJ	MYNN	YSU	MYJ	MYNN	YSU	MYJ	MYNN
Cabauw tower										
Temp. (K)	May	−0.98	−1.61	−1.39	1.31	1.77	1.55	1.72	2.32	2.01
	June	−1.23	−1.64	−1.69	1.55	1.89	1.93	2.04	2.44	2.52
	July	−1.78	−2.19	−2.15	2.10	2.41	2.39	2.66	3.00	2.95
	August	−0.23	−0.95	−0.64	0.83	1.23	1.03	1.17	1.72	1.47
	September	−1.23	2.37	−1.83	1.40	2.39	1.88	1.92	3.12	2.46
All-month average		−1.09	−1.75	−1.54	1.44	1.94	1.76	1.90	2.52	2.28
Wspd ($\mathrm{m\,s^{-1}}$)	May	0.30	0.14	0.25	1.31	1.22	1.24	1.92	1.76	1.80
	June	−0.01	0.15	0.10	0.98	1.02	1.05	1.41	1.48	1.46
	July	0.04	0.14	0.25	1.05	1.04	1.14	1.52	1.48	1.63
	August	0.26	0.15	0.25	1.09	1.09	1.16	1.61	1.58	1.65
	September	0.03	0.13	0.35	1.07	1.04	1.15	1.51	1.54	1.66
All-month average		0.12	0.14	0.24	1.10	1.08	1.15	1.59	1.57	1.64
Sp. hum ($\mathrm{g\,kg^{-1}}$)	May	−0.17	0.15	0.07	0.49	0.68	0.55	0.69	0.93	0.78
	June	−0.23	0.10	0.02	0.68	0.80	0.71	0.94	1.16	1.04
	July	−0.15	0.36	0.06	0.78	1.03	0.87	1.09	1.40	1.21
	August	−0.19	−0.04	−0.06	0.53	0.61	0.54	0.73	0.86	0.76
	September	−0.37	−0.18	−0.21	0.65	0.77	0.66	0.90	1.07	0.92
All-month average		−0.22	0.08	−0.02	0.63	0.78	0.67	0.87	1.08	0.94
Egmond aan Zee mast										
Temp. (K)	May	−1.03	−1.34	−1.21	1.36	1.56	1.47	1.83	2.03	2.02
	June	−1.09	−1.30	−1.38	1.42	1.52	1.61	1.82	1.96	2.11
	July	−1.59	−1.72	−1.68	1.95	2.03	2.02	2.52	2.54	2.55
	August	0.39	−0.26	0.19	0.65	0.71	0.64	0.85	0.94	0.83
	September	−0.83	−1.71	−1.13	1.14	1.84	1.34	1.43	2.31	1.66
All-month average		−0.83	−1.27	−1.04	1.30	1.49	1.42	1.69	1.96	1.83
Wspd ($\mathrm{m\,s^{-1}}$)	May	−0.01	0.02	0.09	1.54	1.62	1.46	2.14	2.28	2.06
	June	−0.17	0.22	−0.09	1.41	1.60	1.57	1.93	2.14	2.16
	July	−0.07	0.18	0.00	1.46	1.55	1.56	1.92	2.10	2.06
	August	0.29	0.07	−0.03	1.25	1.35	1.27	1.69	1.90	1.80
	September	−0.06	0.13	−0.02	1.23	1.34	1.27	1.70	1.88	1.78
All-month average		0.00	0.12	−0.01	1.38	1.49	1.43	1.88	2.06	1.97

© 2014 The Authors. *Quarterly Journal of the Royal Meteorological Society* published by John Wiley & Sons Ltd on behalf of the Royal Meteorological Society.

Consequently, there are no systematic increases or decreases in error associated with time of day, unlike at Cabauw. This is to be expected due to the differences in heat capacity between land and sea.

Summary error statistics for the model simulations at Egmond aan Zee mast are shown in Table 2. In the offshore environment, temperature is again underestimated, with the exception of the YSU and MYNN simulations in August. The MYJ PBL scheme performs relatively poorly in the offshore environment. The YSU PBL scheme has the lowest statistical error scores for temperature.

For wind speed, the MYJ PBL scheme overestimates during all months, whereas with the exception of August the YSU scheme underestimates wind speed at the Egmond aan Zee mast. No scheme consistently outperforms another in terms of mae and rmse for wind speed, in contrast with the Cabauw tower observations. However, the MYJ PBL is consistently poorer than either the YSU or the MYNN at simulating wind speed in terms of mae and rmse.

3.3. *Summary of model evaluation*

In summary, the model error statistics in both the onshore and offshore environments at Cabauw and Egmond aan Zee reveal that no PBL scheme is consistently more accurate than another in terms of overall performance. Referring back to Figure 2, there are three main purposes of the WRF model simulations. Firstly, to quantify the 925 hPa gradient wind speed and direction relative to a specific coastline. Secondly, to determine the magnitude of the land–sea thermal contrast and, thirdly, to generate composite windfields for each sea-breeze type.

Since with the observations available it is not possible to reliably validate wind speeds at 925 hPa as radiosondes offer insufficient temporal frequency, more weight must be given to the ability of the model to simulate 2 m temperature. Therefore the YSU PBL scheme is chosen for use in the WRF model climatological simulations. In keeping with the idealized WRF model simulations of Steele *et al.* (2013), the 925 hPa composite gradient wind speed upper limits are chosen to be $9\,\mathrm{m\,s^{-1}}$ for *pure* sea breezes and $5\,\mathrm{m\,s^{-1}}$ for those of the *backdoor* type.

4. Sea-breeze climatologies

4.1. *Annual and seasonal variability*

Based on the identification of modelled sea breezes on five coastlines, sea-breeze annual frequencies and seasonal distribution are shown in Figure 5 and total sea-breeze frequencies are summarised in Table 3. The total number of sea breezes on each coast varies by over a factor of 2. For example, while 154 sea-breeze events are simulated off the southern coast of Kent, the method identified 335 events on the coast of East Norfolk. The range of *pure*, *corkscrew* and *backdoor* sea-breeze frequencies identified is also remarkably high between coasts. The number of *pure* sea-breeze events, for example, ranges from 21 on the south coast of Kent to 166 off the coast of East Norfolk. While 76 *corkscrew* sea breezes were identified in association with the coast of the Netherlands, 169 *corkscrew* sea breezes were simulated on the East Norfolk coast.

Backdoor sea breezes are the least common of all types. No *backdoor* sea breezes were identified as forming off the coast of East Norfolk, due to the northerly direction of the gradient wind required to produce them. Typically, northerly winds are accompanied by lower air temperatures and potentially convective cloud and so it is likely that this suppresses the land temperature and prevents a sufficient land–sea thermal contrast from developing.

There are no sea-breeze climatological studies, other than for *pure* events, with which to compare these frequencies. Furthermore filter methods are conservative, meaning that, apart from *corkscrew* sea breezes, it is possible that the strict limitation on gradient wind speed could falsely reject days on which sea breezes occur. However, during an observational campaign in southern England between 1962 and 1973, Simpson *et al.* (1977) observed 76 *pure* sea-breeze events. This, combined with the sensitivity tests of Steele (2013) and the presence of sea-breeze features in the composites presented in section 4.2, adds to the confidence that few events are missed.

The most common weather type for producing sea breezes of all types on all coasts is *pure anticyclonic* (A), however the position of the anticyclone relative to the target coastline varies for each sea-breeze type. As a result, there are inter-relationships between sea-breeze types forming on more than one coastline (Table 4). For example, 94% of *backdoor* sea-breeze events on the North Norfolk coast were coincident with *pure* sea breezes on the East Norfolk coast. By contrast, the number of *pure* sea-breeze events forming on the East Norfolk coast are not so strongly associated with *backdoor* sea-breeze events on the coast of North Norfolk (166 versus 51). The fundamental reason for this discrepancy is the tighter restrictions on simulated gradient wind speed (Filter Stage 3; Figure 2). A simulated gradient wind speed restriction of $5\,\mathrm{m\,s^{-1}}$ is imposed on *backdoor* sea breezes compared with $9\,\mathrm{m\,s^{-1}}$ for the *pure* type (Steele *et al.*, 2013). On average, the SST varies between North and East Norfolk by less than 0.5 K and does not account for the large difference in sea-breeze frequency between coasts.

Season length also differs between coasts. A typical Northern Hemisphere sea-breeze season is between May and September, with higher frequencies occurring in June when there is maximum temperature contrast between land and sea (Simpson *et al.*, 1977). However, results for the coasts of East Norfolk, Suffolk and Essex and for the coast of the Netherlands show that sea breezes can occur as early as March and, in the cases of East Norfolk and Suffolk and Essex, as late as October (Figure 5). In terms of wind energy and weather forecasting applications, it is important to know that the season length can vary from coast to coast so that this can be taken into account when, for example, either siting a wind farm or providing a forecast for a sailing event. The strong intercoastal relationship between sea-breeze types is an important factor for weather forecasting in the coastal zone.

It must be noted that, since the completion of the full sea-breeze model climatology using WRF version 3.3.1, a coding bug was found in the YSU scheme which caused excessively strong mixing in the nocturnal PBL (Hu *et al.*, 2013; Sterk *et al.*, 2013). Nevertheless, the skill demonstrated by the YSU scheme in simulating 2 m temperature was still higher in this study than for the other schemes tested. With the implementation of a fix to the coding bug since the release of WRF version 3.4.1, we conducted sensitivity tests using WRF version 3.5 to check whether our results were affected. The tests consisted of applying the sea-breeze identification method to monthly WRF simulations, from May to September 2006, and comparing the sea-breeze frequencies to those found using WRF version 3.3.1. The results revealed that the number of sea-breeze events were the same, and so we are confident that the results presented here are unaffected by this coding bug.

4.2. *Sea breeze composites*

One measure of the ability of the filter method to realistically capture sea-breeze events is to examine whether sea-breeze features are evident in composite imagery. As an example, Figure 6 shows the composite average of 10 m divergence at 1600 UTC for the 166 *pure* sea-breeze events identified as forming off the coast of East Norfolk. Clearly evident is a convergence line which is indicative of a sea-breeze front between 10 and 15 km inland. Note that the change in coastal orientation in the northern and southern sectors of the coast of East Norfolk causes the sea breeze in these regions to take on different characteristics. These characteristics of the *backdoor* and *corkscrew* sea breezes will be explored further in sections 4.2.2 and 4.2.3. The coherence of

© 2014 The Authors. *Quarterly Journal of the Royal Meteorological Society* published by John Wiley & Sons Ltd on behalf of the Royal Meteorological Society.

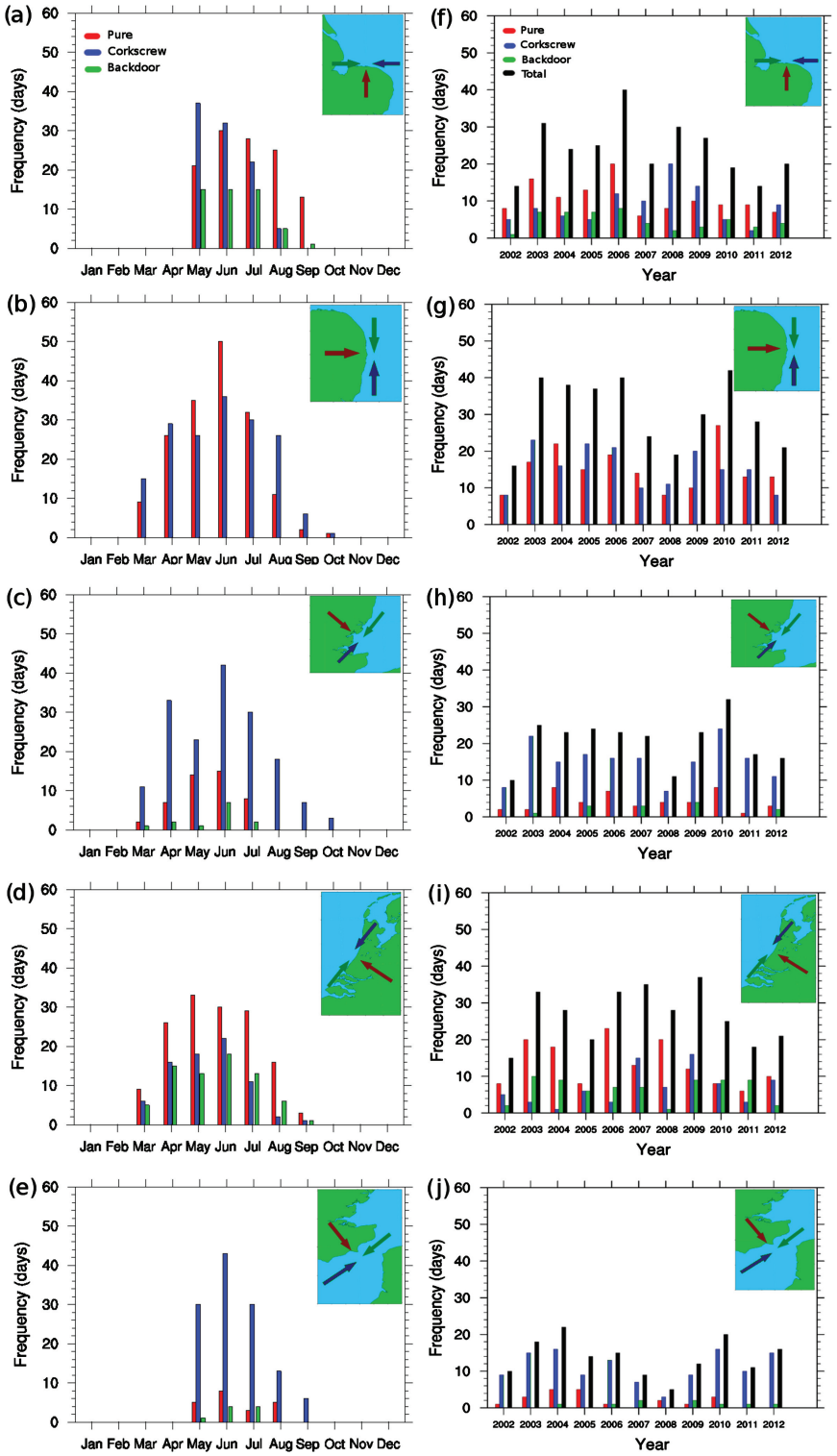

Figure 5. Monthly frequencies of sea breezes simulated on the coasts of (a) North Norfolk, (b) East Norfolk, (c) Suffolk and Essex, (d) the Netherlands and (e) South Kent, and (f)–(j) year-to-year variation of sea breezes simulated on the corresponding coasts. The arrows (color in online) represent the gradient wind direction required to produce each sea-breeze type.

the convergence line (Figure 6) combined with the characteristic temporal evolution of the surface composite windfields in all composites (e.g. Figure 7) give added confidence that the method is correctly identifying sea-breeze days.

4.2.1. *Pure sea breezes*

The simplest coastline to consider is the coast of East Norfolk as its central stretch is relatively straight and the nearest opposing coastline is approximately 250 km offshore. Interference from opposing coasts is therefore less than for other coasts. Before the initiation of the 166 *pure* sea-breeze events on the East Norfolk coast, calm zones are formed between 0 and 30 km offshore (Figure 7). In this study, calm zones are defined as regions where the simulated 10 m wind speed is less than 1 m s^{-1}. Calm zones are formed as the result of thermally induced low-level pressure gradients opposing the offshore gradient wind. Typically, as the land–sea thermally induced pressure gradient overcomes the synoptic pressure gradient to form the sea breeze, the calm zones start at the shoreline and are forced offshore as the sea breeze develops (e.g. Figures 7 and 8; Appendix S1, Figure S3).

Where there are variations in coastal orientation or the presence of another coastline, the offshore windfields are more complex. The shape of the Dutch coast is concave, implying that the

© 2014 The Authors. *Quarterly Journal of the Royal Meteorological Society* published by John Wiley & Sons Ltd on behalf of the Royal Meteorological Society.

Table 3. Frequency (days) of sea breezes for each coastline between January 2002 and December 2012.

Coast	*Pure*	*Corkscrew*	*Backdoor*	Total
North Norfolk	117	96	51	264
East Norfolk	166	169	0	335
Suffolk+Essex	46	167	13	226
Netherlands	146	76	71	293
South Kent	21	122	9	154
Total	496	630	144	1270

orientation of the coastline with respect to the gradient wind changes with location along the coast. In this case, no calm zones are formed. To the north of the Dutch coast, the angle of the coastline with respect to the gradient wind is sufficient to form a region of divergence, altering the characteristics of the sea breeze (Appendix S1, Figure S4).

Increasing the coastal complexity further still by a second coastline such as one adjacent (North Norfolk) or opposite (Southern Kent, Suffolk and Essex) has further impact on the timing, location and extent of offshore calm zones. Adjacent to the coast of North Norfolk, to the northwest, lies the coast of Lincolnshire (Figure 3(b)) which produces *corkscrew* type sea breezes when the orientation of the gradient wind is favourable for developing *pure* sea breezes on the North Norfolk coast (Figure 8). The result is that the calm zone is initially (1000 UTC) located in the eastern part of the North Norfolk coast and migrates further west (1200 UTC) towards the Wash through a combination of the *corkscrew* sea breeze on the East Norfolk coast and the initialization of the *pure* sea breeze off the coast of North Norfolk.

The coast of South Kent formed the fewest *pure* sea breezes during the study period (Table 3). At 1000 UTC, several distinct calm zones are present including one which spans the length of the Strait of Dover (Appendix S1, Figure S5). This composite *pure* sea breeze is stronger than the *pure* sea breeze on the other coastlines and is also the only *pure* sea breeze to form a coastal jet. These jets are more typically associated with *corkscrew* sea breezes, described next.

4.2.2. *Corkscrew sea breezes*

The most common distinguishing feature of the *corkscrew* sea breeze is the formation of a coastal jet. These jets are apparent

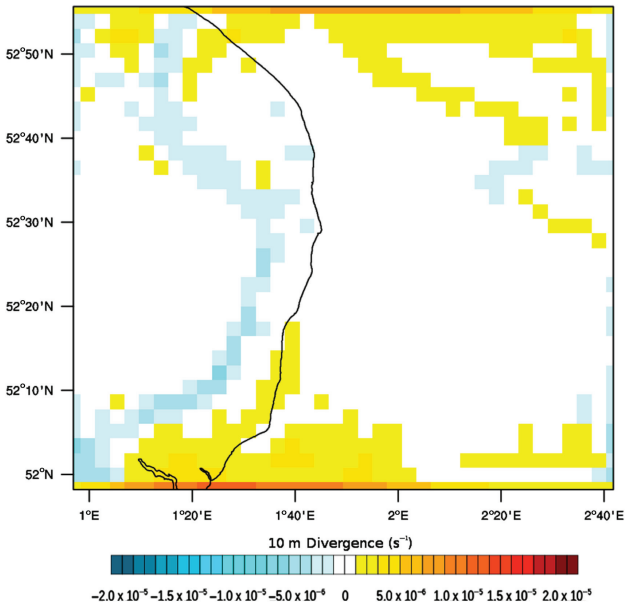

Figure 6. 1600 UTC divergence composite for the 166 *pure* sea-breeze events forming on the East Norfolk coast. Filled boxes indicate 10 m divergence (s^{-1}). Negative values imply convergence.

on all coastlines with the exception of the coast of Suffolk and Essex. Coastal jets are defined as local wind speed maxima which are within 1 km of a coastline (Capon, 2003; Hunt *et al.*, 2004). Their horizontal extent can range between 30 and 300 km and so the *corkscrew* sea-breeze influence has greater potential to impact other coastlines further offshore. They have numerous causes (Hunt *et al.*, 2004), the most relevant to the *corkscrew* sea breeze being when Coriolis force acts on a shore-parallel flow with the land surface to the left (in the Northern Hemisphere). A *detached* jet is formed where there is a coastal discontinuity present, such as a headland or bay. Finally, if there is a significant topographic barrier, such as the coast of East Greenland, then a *barrier* jet may form (e.g. Moore and Renfrew, 2005).

The Dover Strait Jet (Capon, 2003; Hunt *et al.*, 2004) is prevalent after 1200 UTC in the composites of the *pure* and *corkscrew* (Figure 9) sea breezes forming off the coast of South Kent, but not in the *backdoor* composite, though another jet forms off the coast of northern France in the opposing direction which is also indicative of a *corkscrew* sea breeze. Further analysis

Table 4. The relationship between sea-breeze types identified on different coastlines.

Coast	Type	North Norfolk			East Norfolk			Suffolk+Essex			Netherlands			South Kent		
		p	c	b	p	c	b	p	c	b	p	c	b	p	c	b
North Norfolk	p	–	–	–	0	86	0	0	35	0	30	2	12	0	19	2
	c	–	–	–	0	0	0	0	0	10	40	39	1	0	0	7
	b	–	–	–	94	0	0	20	61	0	0	0	37	4	49	0
East Norfolk	p	0	0	29	–	–	–	25	50	0	0	0	17	7	47	1
	c	60	0	0	–	–	–	0	41	0	31	1	15	0	15	0
	b	0	0	0	–	–	–	0	0	0	0	0	0	0	0	0
Suffolk + Essex	p	0	0	22	89	0	0	–	–	–	0	7	24	52	0	0
	c	25	0	19	50	42	0	–	–	–	7	0	21	0	38	0
	b	0	77	0	0	0	0	–	–	–	15	77	0	0	0	31
Netherlands	p	24	26	0	0	36	0	0	8	1	–	–	–	0	3	3
	c	3	49	0	0	3	0	0	0	13	–	–	–	0	0	5
	b	20	1	27	41	35	0	4	49	0	–	–	–	0	31	0
South Kent	p	0	0	10	57	0	0	52	0	0	0	0	0	–	–	–
	c	18	0	20	64	14	0	20	52	0	4	0	18	–	–	–
	b	22	78	0	0	22	0	0	0	0	44	56	44	–	–	–

Values are expressed as percentages of the number of sea breezes occurring on the coastlines in the far left column.
p = *pure*, c = *corkscrew* and b = *backdoor*.

© 2014 The Authors. *Quarterly Journal of the Royal Meteorological Society* published by John Wiley & Sons Ltd on behalf of the Royal Meteorological Society.

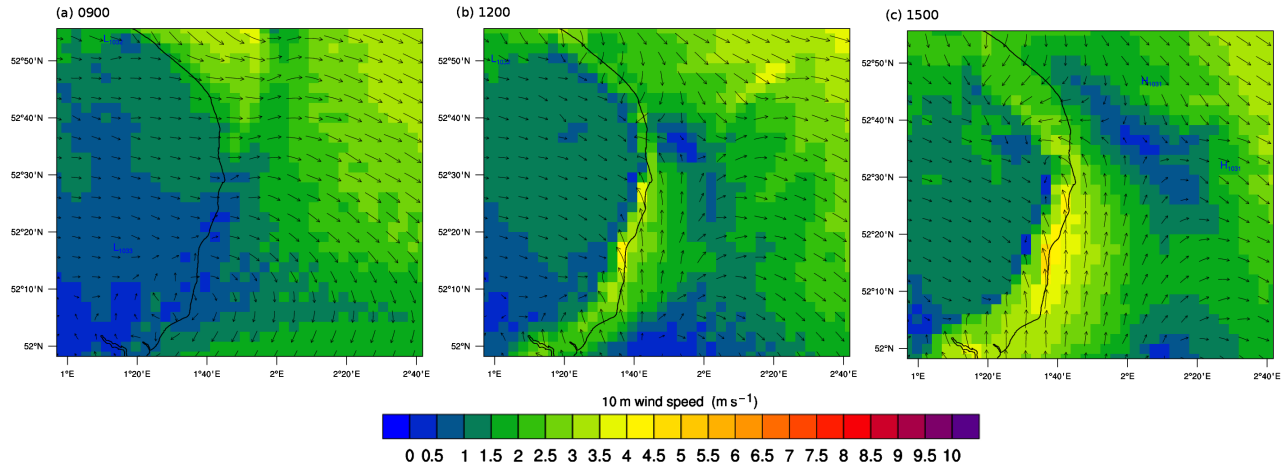

Figure 7. Composite 10 m wind speed (shading, m s^{-1}) and direction (arrows) of the 166 simulated *pure* sea-breeze events identified on the East Norfolk coastline by the filter method at (a) 0900 UTC, (b) 1200 UTC and (c) 1500 UTC.

of the results for the coasts of Suffolk and Essex reveals that, although the 925 hPa winds are southwesterly, as should be the case with *corkscrew* events, the 10 m wind direction remains northeasterly for the duration of the composite simulation. Therefore the surface winds are not conducive for the formation of a surface jet.

The 10 m simulated wind speed at the core of each jet is between 7 and 8 m s^{-1}, whilst onshore the wind speed is between 5 and 6 m s^{-1}. Without the inclusion of the jet, which would require a third dimension, the differences between the *pure* and *corkscrew* sea-breeze 10 m wind speeds are in keeping with the 2D idealized results of Steele *et al.* (2013).

Importantly, the higher simulated 10 m wind speeds present in the *corkscrew* sea-breeze events impact sea breezes of different types on other coastlines. For example, the impact of the *corkscrew* circulations which form on the coasts of Lincolnshire and East Norfolk in conjunction with the *pure* sea breeze on the coast of North Norfolk. Once the *corkscrew* sea breezes establish coastal jets after 1200 UTC (Figure 8), they dominate the offshore environment and negate the impact of the *pure* sea breeze on the North Norfolk coast.

4.2.3. *Backdoor sea breezes*

Backdoor sea breezes are associated with lower simulated 10 m wind speeds than the other sea-breeze types. They are also associated with offshore calm zones, although in many cases the 10 m windfield is predominantly calm and so the effect of the *backdoor* sea breeze is to reduce the near-shore extent of the calm zones as the *backdoor* sea breeze intensifies.

The strength of the onshore flow of the sea breeze is the weakest of the sea-breeze types simulated, reaching 10 m simulated wind speeds of between 2 and 3 m s^{-1}. In the offshore environment, like the composite *pure* sea-breeze evolution on the coast of North Norfolk (117 events), the *backdoor* sea breeze is subject to impact from *corkscrew* sea breezes forming on nearby coastlines. This occurs for both the 13 and 9 *backdoor* sea-breeze events respectively on the South Kent and the Suffolk and Essex coastlines; however it is also noted that *backdoor* sea breezes are not common events on these coastlines during the 11 year study period.

5. Wind energy applications

Offshore wind turbines typically have a hub-height cut-in speed of 4 m s^{-1} (4C Offshore, 2014). Furthermore, the wind power generated by a turbine is proportional to the cube of the wind speed and so features such as offshore calm zones, coastal jets and the sea-breeze onshore flow all have the potential to significantly impact wind power generation. Sudden changes in power generation are known as ramp-up or ramp-down events, depending on the sign of the change. Unanticipated ramp-up and ramp-down events can be very difficult for electrical grid operators to manage (Dragoon, 2010).

In this next section, we apply a typical power curve to the modelled sea breeze composite wind speeds and compare with observations at Egmond aan Zee wind farm (Figure 3(b)) to determine the temporal impact of each sea-breeze type on wind power output. To quantify the spatial impact, we calculate the capacity factor, which is defined as the ratio of power output to the theoretical maximum power produced by a turbine in a given time period. Wind speeds are taken from the fourth model level, at approximately 90 m, for spatial analyses, but for comparisons with observations the wind speeds are interpolated to the height of the measurements.

5.1. *Temporal evolution*

The Egmond aan Zee meteorological mast was in operation between 2005 and 2010. During this time, the sea-breeze filter method identified 77 *pure*, 52 *corkscrew* and 34 *backdoor* sea breezes forming on the coast of the Netherlands. Figure 10 shows the typical diurnal cycle of power output for each sea breeze type at the Egmond aan Zee mast. In this case, a power curve (Appendix S1, Figure S6) is fitted for a 3.6 MW turbine with a hub height and blade radius of 70 and 60 m respectively. These specifications are typical for current wind turbines installed in the southern North Sea.

The wind power diurnal cycle associated with the 77 *pure* sea-breeze events (Figure 10(a)) reveals a morning decline in power output by approximately 0.8 MW due to the reduction in simulated wind speed associated with establishment of the thermally induced pressure gradient prior to sea-breeze onset. Once the sea breeze reaches the Egmond aan Zee wind farm at approximately 1200 UTC, the gain in attributable power is approximately 1.3 MW. The model performance is good to the extent that the magnitude of the increase in wind power is approximately equal to the observations and the diurnal cycle is well captured, though there is a general overestimation in power output by the WRF model during these days.

The composite wind power diurnal cycle of the 52 *corkscrew* sea-breeze events (Figure 10(b)) reveals that there is a net power gain of 2.0 MW in relation to the power output prior to 0900 UTC associated with the arrival of the *corkscrew* sea breeze. The power output is again simulated well in the period 0000–0800 UTC but the WRF model somewhat overestimates the effect of the sea breeze and the thermal pressure gradient after 1000 UTC.

© 2014 The Authors. *Quarterly Journal of the Royal Meteorological Society* published by John Wiley & Sons Ltd on behalf of the Royal Meteorological Society.

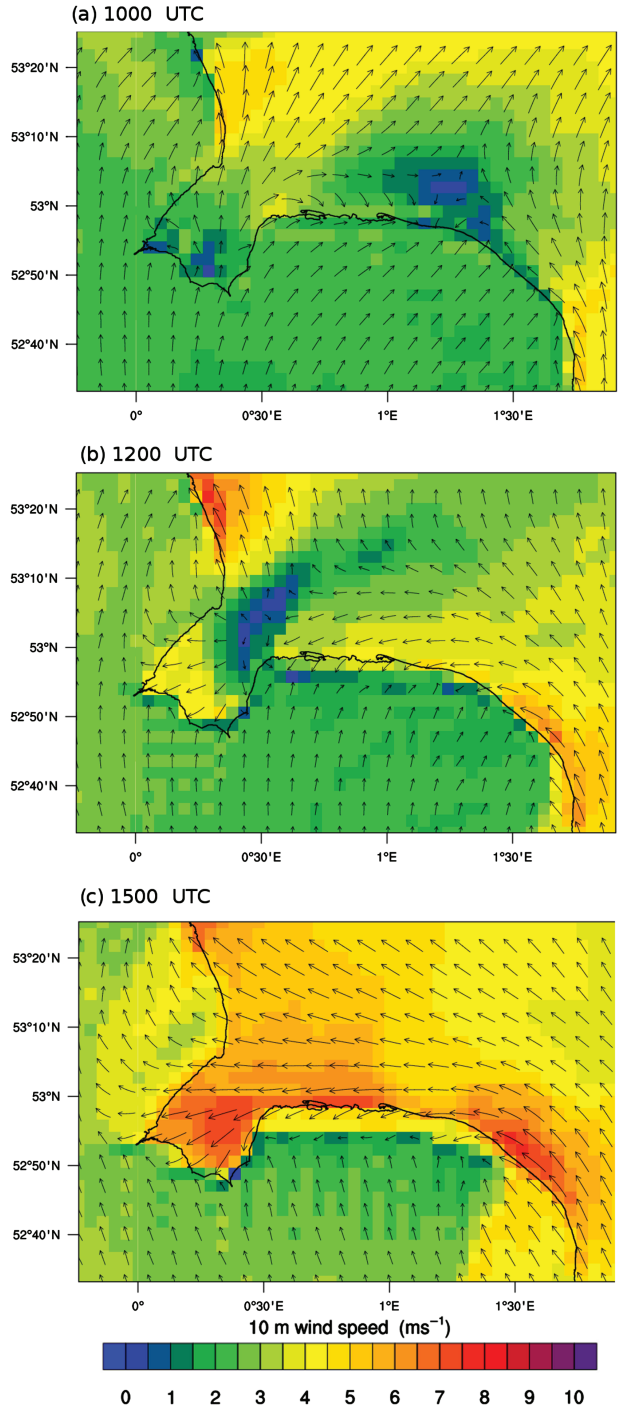

Figure 8. As Figure 7, but for the 117 simulated *pure* predicted sea-breeze days for the coast of North Norfolk at (a) 1000 UTC, (b) 1200 UTC and (c) 1500 UTC.

As the 34 *backdoor* sea-breeze events occur during periods of relatively low wind speed, the power output recorded at any one time is never higher than 0.5 MW (Figure 10(c)). The composite diurnal cycle also does not show a pronounced maximum associated with the arrival of the sea breeze, though a change in wind direction is present (not shown).

Wind speed shear across the turbine blades is an important parameter for the wind energy industry. Increased wind speed shear can both reduce the performance of a wind turbine as well as increase the stress on the blades. Figure S7 in Appendix S1 shows the composite wind speed shear between 21.6 and 116 m at the Egmond aan Zee offshore wind farm. Both the composite *pure* and *corkscrew* sea-breeze wind speed shear diurnal cycles are stronger than the composite of the non-sea-breeze events by 0.5–0.7 m s^{-1}. They are also more variable. The variation of the composite wind speed shear diurnal cycle of the 77 *pure* and 52 *corkscrew* sea-breeze events is approximately 0.7 m s^{-1} compared with 0.4 m s^{-1} for non-sea-breeze days. However, these values are still relatively small and so would not be expected to have a significant impact on turbine performance (Elliott and Cadogan, 1990).

The results presented thus far are for turbines which are currently operational in the southern North Sea. Projections of turbine size indicate that, by 2020, it is possible that 8 MW turbines with hub heights exceeding 100 m and blade radii of 80 m will be operational (Bilgili *et al.*, 2011) and so we now conduct further analysis to vary turbine parameters accordingly. Figure 11 shows wind power calculated at 116 m height for each of the sea-breeze types at the Egmond aan Zee meteorological mast assuming an 8 MW turbine with blade radius of 80 m. The higher power rating of the 8 MW turbine causes the turbine power output to become more sensitive to simulated wind speed changes than the smaller 3.6 MW design. Consequently the impact of each sea-breeze type is greater for the 8 MW turbine, suggesting that power output will become more sensitive to sea breezes in the future.

5.2. *Spatial differences*

In order to determine the spatial impact of the sea breeze on wind energy, it is necessary to define what constitutes a *non-sea-breeze* day in such a way that the impact of the sea breeze is not masked by other meteorological phenomena. Here, we utilize the identification method by defining a non-sea-breeze day as one which passes all filters apart from the strength of the land–sea contrast (Filter 4; Figure 2). This way, a close approximation of the meteorological conditions of a sea-breeze day is achieved without a sea breeze forming. A composite of all non-sea-breeze events smooths out any day-to-day variability and so the impact of the sea breeze can be isolated by a subtraction of composite sea-breeze and non-sea-breeze events.

As *backdoor* sea breezes form in very light simulated wind speeds that are close to the wind turbine cut-in threshold of 4 m s^{-1}, there is very little benefit in power generation on these days except during the early afternoon once the sea breeze has established. Indeed, in comparison with the predicted non-sea-breeze days for each coastline, there is no difference in capacity factor. However, Figure 12 shows the composite capacity factor difference between the 13 *backdoor* sea breezes on the Suffolk and Essex coast and the equivalent composite of 18 non-sea-breeze days. Referring to Table 4, the orientation of the gradient wind for the 13 *backdoor* sea-breeze events on this coast is also favourable for *corkscrew* sea breezes on the coast of the Netherlands. The impact of this *corkscrew* sea breeze is clearly affecting the coast of East Norfolk and parts of Suffolk.

The *corkscrew* sea breeze gives a net contribution to capacity factor of between 10 and 15%, due to the increase in wind speed associated with the coastal jets (Figure 13). The offshore extent of these differences is well within the range of the newly proposed Round 3 developments in the central southern North Sea (RenewableUK, 2014). Furthermore, the effect of the *corkscrew* sea breeze forming on the Lincolnshire coast on the *pure* type forming on the coast of North Norfolk is clearly evident in the capacity factor differences.

As reported in the comparisons with the Egmond aan Zee mast, net gains in wind power are small for *pure* sea breezes. Figure 14 shows the instantaneous wind power differences between predicted sea-breeze and non-sea-breeze days, for the 21 *pure* events forming on the coast of South Kent at 0600 and 1200 UTC. Sea breezes are clearly forming off the coast of the UK at 1200 UTC, giving confidence in the method to differentiate between sea-breeze and non-sea-breeze days. Also, there are small power gains of approximately 0.5 MW up to 6 km offshore from the South Kent coast. There are no differences between instantaneous wind power within the

© 2014 The Authors. *Quarterly Journal of the Royal Meteorological Society* published by John Wiley & Sons Ltd on behalf of the Royal Meteorological Society.

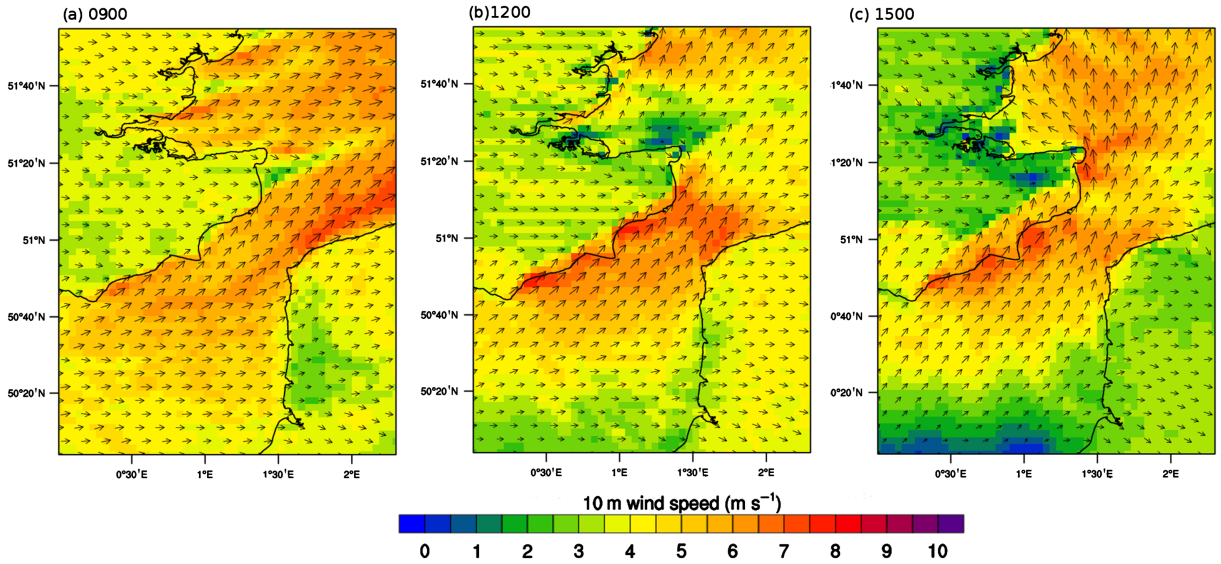

Figure 9. As Figure 7, but for the 122 simulated *corkscrew* sea-breeze events identified on the South Kent coast at (a) 0900 UTC, (b) 1200 UTC and (c) 1500 UTC.

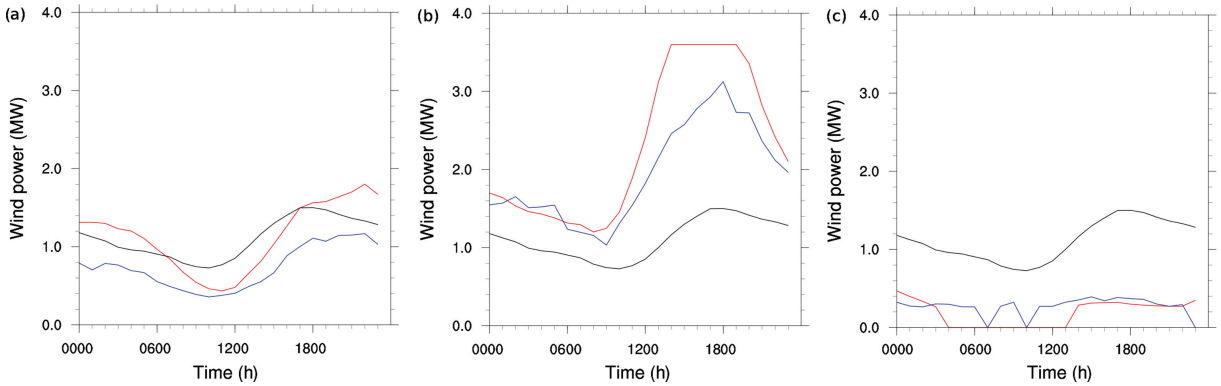

Figure 10. Composite wind power diurnal cycle (UTC) of (a) 77 *pure*, (b) 52 *corkscrew* and (c) 34 *backdoor* sea-breeze events, between 2005 and 2010, at the Egmond aan Zee offshore wind farm. Composite observations (blue lines) of 70 m wind speed were converted into wind power estimates using a theoretical 3.6 MW turbine with blades of radius 60 m. Red lines represent the simulated composite 3 km WRF model power output converted from wind speed using the same theoretical turbine as the observations. The simulated composite wind power diurnal cycle of non-sea-breeze days are shown in black.

sea-breeze circulation and the composite instantaneous wind power of the 143 non-sea-breeze events within 50 km of the coastline.

Ahead of the sea breeze in the offshore environment, there is a region where there is a drop in power output by approximately 1 MW associated with the drop in wind speed ahead of the sea breeze (Figure 14). Generally, the predicted non-sea-breeze days for the *pure* sea-breeze type forming on the coast of South Kent produce a larger power than the composite of the 21 *pure* sea-breeze events on the same coastline. This results in a capacity factor difference of approximately 10% over open water (Figure 15). Where the *pure* sea breeze is present, the capacity factor difference is cancelled out.

6. Summary and conclusions

A new sea-breeze identification method which incorporates the little-known different sea-breeze types and which is adaptable for any coastline has been tested on five different coasts in the southern North Sea between 2002 and 2012. Furthermore,

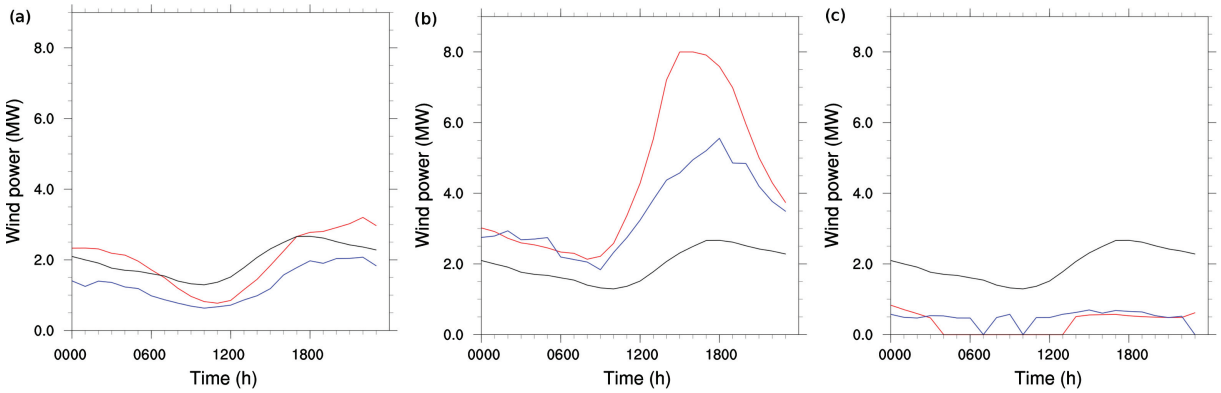

Figure 11. As Figure 10, but measurements of 116 m wind speed (blue) were converted into wind power estimates using a theoretical 8 MW turbine with blades of radius 80 m.

© 2014 The Authors. *Quarterly Journal of the Royal Meteorological Society* published by John Wiley & Sons Ltd on behalf of the Royal Meteorological Society.

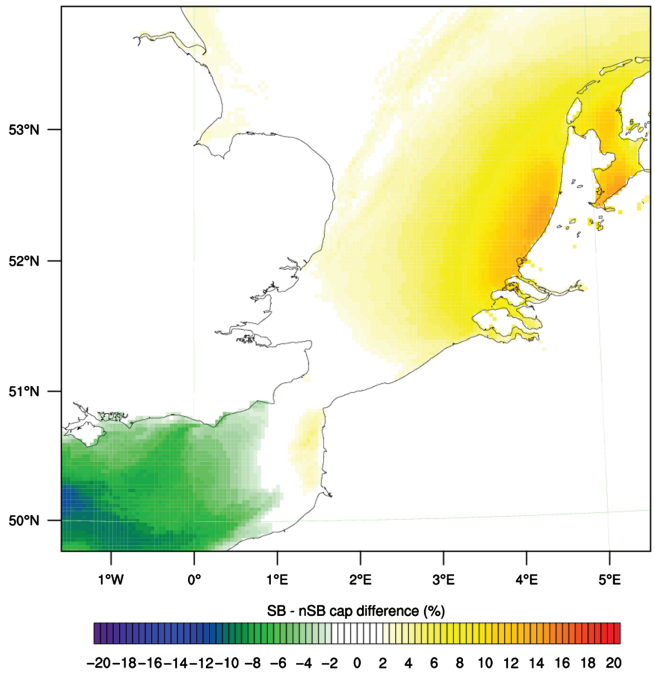

Figure 12. Composite capacity factor difference of the 13 *backdoor* sea breezes (SB) forming on the coast of Suffolk and Essex from the 18 days which were rejected (nSB) on the basis of a temperature contrast greater than 0 but less than 5 K. The capacity factors are calculated over the composite 24 h period.

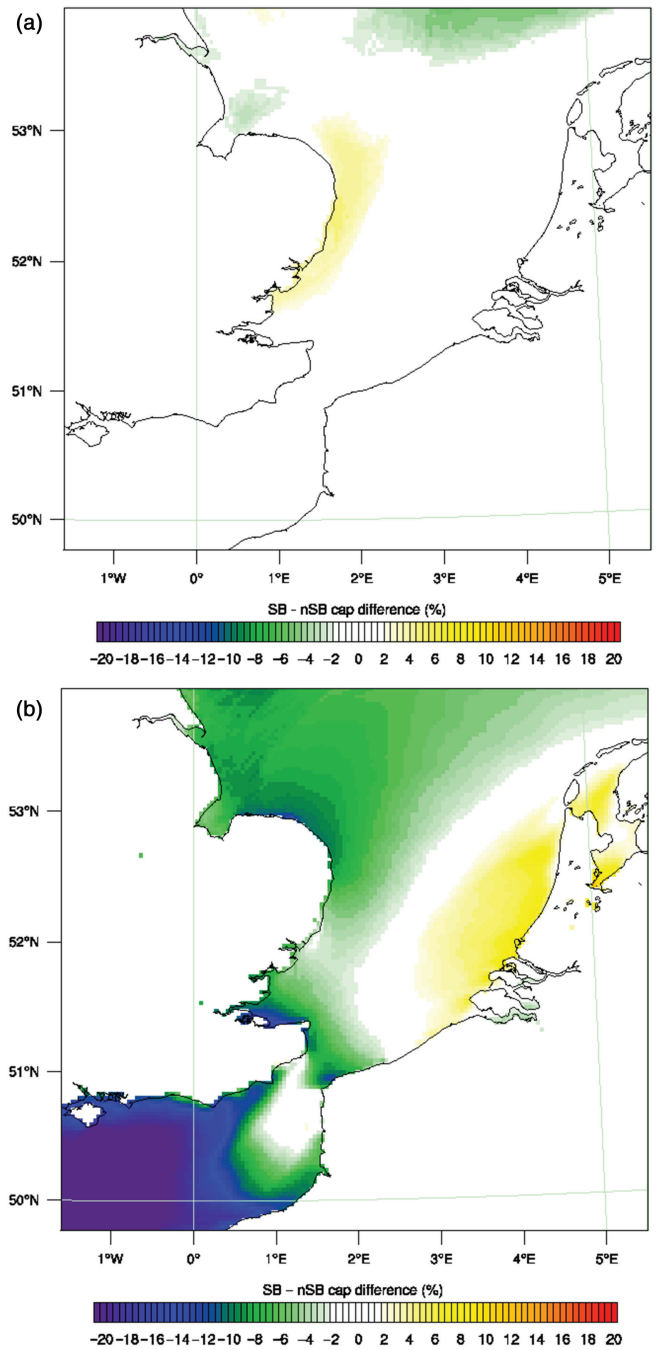

Figure 13. Composite capacity factor difference between both the 167 and 76 *corkscrew* sea breeze events (SB) forming on the coasts of (a) Suffolk and Essex and (b) the Netherlands from the days which were rejected (nSB) on the basis of a temperature contrast greater than 0 but less than 5 K (580 and 190 rejected days respectively). The capacity factors are calculated over the composite 24 h period.

in the process of constructing the climatology, three different PBL physics schemes were verified against meteorological mast measurements onshore and offshore of the coast of the Netherlands. The composite windfields were subsequently used to quantify the effects associated with each type on offshore wind farms, both in terms of a composite diurnal cycle for each sea-breeze type and in terms of a spatial comparison between predicted sea-breeze and non-sea-breeze days.

The results show a considerable intercoast variability of frequencies and season length between sea-breeze types which is attributable to coastal orientation relative to the prevailing wind direction. Total sea-breeze frequencies can vary by as much as a factor of 2 between nearby coasts, whereas the frequency of individual types can vary by a factor of 3.

Through analysis of the composite windfields, the coherence of the sea-breeze characteristics in composites comprising around 100 events gives a clear indication that the identification method is reliably identifying sea-breeze days. *Pure* sea breezes are found to induce offshore calm zones, defined as regions where the 10 m simulated wind speed is less than 1 m s^{-1}. The horizontal extent, duration and timing of the calm zones is dependent on the complexity of the coastline.

Corkscrew sea breezes are found to induce coastal jets as a result of Coriolis acceleration acting to create a region of divergence along the coast. The presence of these jets is found to influence the wind climate of nearby coasts, such as between North Norfolk and Lincolnshire, and coasts which are greater than 100 km apart, such as the Dutch coast and Suffolk and Essex. *Corkscrew* sea breezes are also found to be the strongest type of sea breezes reaching 10 m simulated wind speeds of approximately 5 m s^{-1}.

Backdoor sea breezes are the least common type to occur between 2002 and 2012 for all coastlines. If present, their development is restricted to lower gradient wind speeds by *corkscrew* sea breezes from nearby coasts impinging on the circulation. Onshore 10 m wind strength is also weakest for this sea breeze type, reaching speeds of between 2 and 3 m s^{-1}.

Awareness of each sea breeze type and their relative characteristics is not widespread in the weather forecasting community and so improved knowledge of the differences between each type, their relative frequencies and intercoastal dependencies can all serve to help a weather forecaster make informed decisions. For instance, knowledge that a *corkscrew* sea breeze rather than a *pure* type is going to form in a sailing event will allow the forecaster to advise stronger winds in the offshore environment.

In relation to wind energy, traditional siting methods often examine a single coastline, though we show here that multiple coastlines within a region need to be taken into account for a single location. The *corkscrew* sea breeze causes a net enhancement to wind energy on a given day of as much as 10% due to the presence of the coastal jet, whereas the *pure* sea breeze only marginally cancels out the effect of the calm zones which are formed prior to sea-breeze onset. *Backdoor* sea breezes form close to the cut-in wind speed of wind turbines, and so it is unlikely that the wind energy industry will utilize predicted *backdoor* sea-breeze days for wind power generation, rather than scheduling maintenance.

© 2014 The Authors. *Quarterly Journal of the Royal Meteorological Society* published by John Wiley & Sons Ltd on behalf of the Royal Meteorological Society.

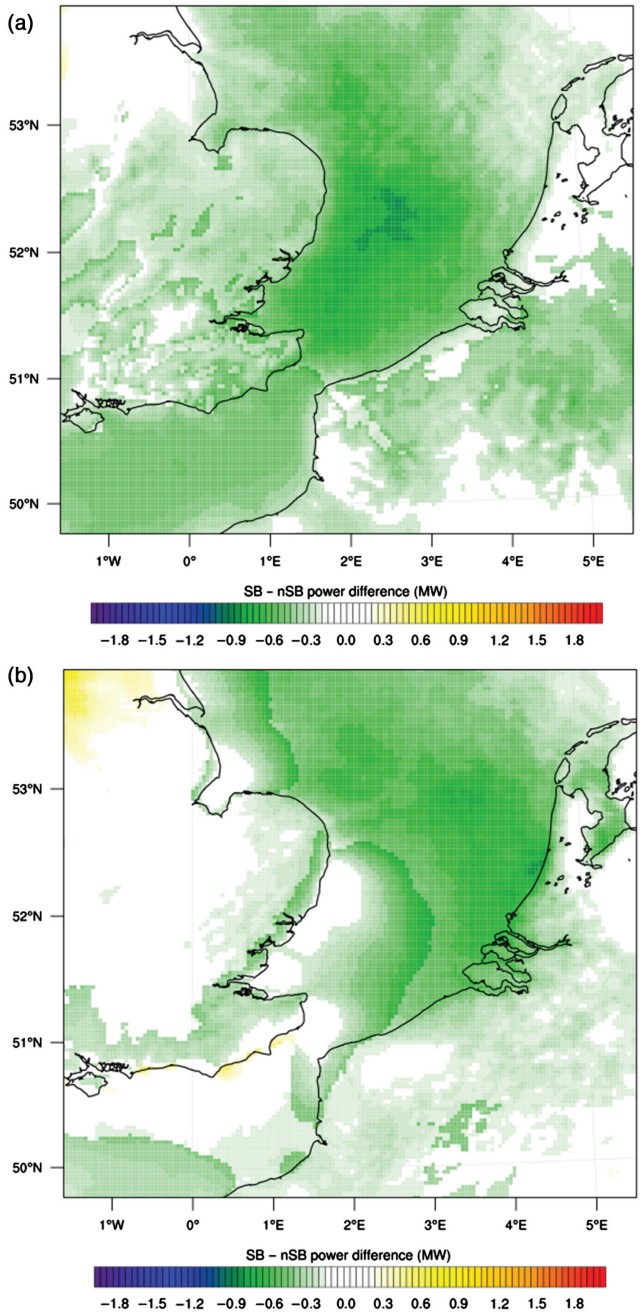

Figure 14. Wind power difference between the 21 *pure* sea breezes (SB) forming off the coast of South Kent with the 143 days which were rejected (nSB) on the basis of a land–sea temperature contrast greater than 0 but less than 5 K at (a) 0600 UTC and (b) 1300 UTC.

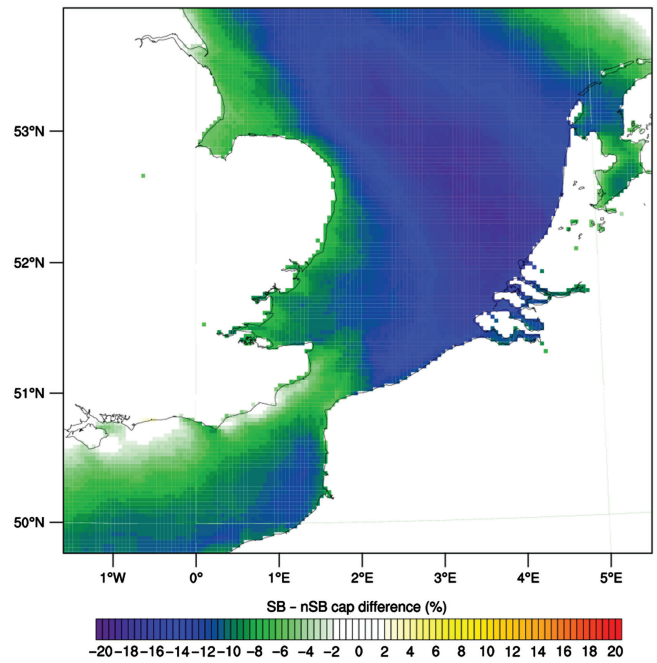

Figure 15. Composite capacity factor difference between the 21 *pure* sea breezes (SB) forming on the coast of South Kent with the 143 days which were rejected (nSB) on the basis of a land–sea temperature contrast greater than 0 but less than 5 K. The capacity factors are calculated over the composite 24 h period.

Furthermore, the effects studied here relate to a single hypothetical wind turbine, rather than a more complex farm. Variations in farm shape and turbine spacing introduce differences in wind power production from each individual wind turbine and so power production is not uniform across the wind farm. Future work will incorporate this to examine, in more detail, the effects of sea breezes to further explore our initial findings. There are also other features, such as the weaker land breeze in the autumn and winter months. These features passed the sea-breeze identification method until Filter 4, but appeared to form calm zones like the sea-breeze counterpart and so would warrant further investigation.

The high degree of interannual variability in sea-breeze events presents a challenge in forecasting and has implications for the choice of typical meteorological years for resource assessment. However, with the advent of larger turbines, the impact of the sea breeze and other similar mesoscale phenomena may be increased in the future as the sensitivity of power output to wind speed is increased by the higher power ratings of the turbines.

Acknowledgements

This work was supported by the Natural Environment Research Council (NERC; grant number NE/H524506/1) through a PhD studentship awarded to CJ Steele. The data produced by the application of the sea-breeze identification method are available for collaborative research, supported by metadata and NCAR Command Language visualization scripts; requests to csteele734@gmail.com. The authors would like to thank NERC and Weatherquest Ltd for providing the funding to make this research possible. Also, the reviewers are thanked for providing such helpful comments on the manuscript during the review process. Finally, we would like to thank Nordzeewind B. V. and the Cabauw Experimental Site for Atmospheric Research (CESAR) consortium for providing the offshore and onshore mast data.

Supporting information

The following supporting information is available as part of the online article:

Appendix S1. Modelling sea-breeze climatologies and interactions on coasts in the southern North Sea: implications for offshore wind energy.

References

4C Offshore. 2014. *Offshore wind Turbine Database*. 4C Offshore Ltd: Lowestoft, UK. http://www.4coffshore.com/windfarms/turbines.aspx (accessed 8 November 2014).

Abbs DJ, Physick WL. 1992. Sea-breeze observations and modelling: a review. *Aust. Meteorol. Mag.* **41**: 7–19.

Arritt RW. 1989. Numerical modelling of the offshore extent of sea breezes. *Q. J. R. Meteorol. Soc.* **115**: 547–570.

Arritt RW. 1993. Effects of the large-scale flow on characteristic features of the sea breeze. *J. Appl. Meteorol.* **32**: 116–125, doi: 10.1175/1520-0450(1993)032<0116:EOTLSF>2.0.CO;2.

Atkinson BW. 1981. *Meso-Scale Atmospheric Circulations*. Academic Press: Waltham, MA.

© 2014 The Authors. *Quarterly Journal of the Royal Meteorological Society* published by John Wiley & Sons Ltd on behalf of the Royal Meteorological Society.

Azorin-Molina C, Chen D, Tijm S, Baldi M. 2011a. A multi-year study of sea breezes in a Mediterranean coastal site: Alicante (Spain). *Int. J. Climatol.* **31**: 468–486.

Azorin-Molina C, Tijm S, Chen D. 2011b. Development of selection algorithms and databases for sea breeze studies. *Theor. Appl. Climatol.* **106**: 531–546, doi: 10.1007/s00704-011-0454-4.

Biggs WG, Graves ME. 1962. A lake breeze index. *J. Appl. Meteorol.* **1**: 474–480.

Bilgili M, Yasar A, Sinmsek E. 2011. Offshore wind farm development in Europe and its comparison with onshore counterpart. *Renewable Sustainable Energy Rev.* **15**: 905–915.

Borne K, Chen D, Nunez M. 1998. A method for finding sea breeze days under stable synoptic conditions and its application to the Swedish west coast. *Int. J. Climatol.* **18**: 901–914.

Brettle M, Smith B. 1999. *Weather to Sail: The Complete Guide to Sailing Weather*. The Crowood Press: Marlborough, UK.

Capon RA. 2003. Wind speed-up in the Dover Straits with the Met Office new dynamics model. *Meteorol. Appl.* **10**: 229–237.

Cheng FY, Chin SC, Liu TH. 2012. The role of boundary-layer schemes in meteorological and air quality simulations of the Taiwan area. *Atmos. Environ.* **54**: 714–727.

Crosman ET, Horel JD. 2010. Sea and lake breezes: A review of numerical studies. *Boundary-Layer Meteorol.* **137**: 1–29, doi: 10.1007/s10546-010-9517-9.

Damato F, Planchon O, Dubreuil V. 2003. A remote-sensing study of the inland penetration of sea-breeze fronts from the English Channel. *Weather* **58**: 219–226, doi: 10.1256/wea.50.02.

Dragoon K. 2010. *Valuing Wind Generation on Integrated Power Systems*. Elsevier: Amsterdam.

EC. 2009. Directive 2009/28/ec of the European Parliament and of the Council: On the promotion of the use of energy from renewable sources and amending and subsequently repealing directives 2001/77/ec and 2003/30/ec. *Off. J. Europ. Union* **140**: 16–62.

Elliott DL, Cadogan JB. 1990. 'Effects of wind shear and turbulence on wind turbine power curves'. In *Scientific Proceedings of European Community Wind Energy Conference and Exhibition*, Madrid, 10–14 September.

Esau I, Byrkjedal Ø. 2007. Application of a large-eddy simulation database to optimisation of first-order closures for neutral and stably stratified boundary layers. *Boundary-Layer Meteorol.* **125**: 207–225, doi: 10.1007/s10546-007-9213-6.

Fichet AD, Quenol H, Planchon O, Douvinet J. 2010. Analysis of local wind systems in the Caen region (lower Normandy, France). *Int. J. Climatol.* **30**: 406–417, doi: 10.1002/joc.1889.

Finkele K. 1998. Inland and offshore propagation speeds of a sea breeze from simulations and measurements. *Boundary-Layer Meteorol.* **87**: 307–329.

Furberg M, Steyn DG, Baldi M. 2002. The climatology of sea breezes on Sardinia. *Int. J. Climatol.* **22**: 917–932, doi: 10.1002/joc.780.

Gahmberg M, Savijarvi H, Leskimen M. 2010. The influence of synoptic scale flow on sea-breeze-induced surface winds and calm zones. *Tellus* **62A**: 209–217.

Golding B, Clark PA, May B. 2005. The Boscastle flood: Meteorological analysis of the conditions leading to flooding on 16 August 2004. *Weather* **60**: 230–235, doi: 10.1256/wea.71.05.

Hong SY, Noh Y, Dudhia J. 2006. A new vertical diffusion package with an explicit treatment of entrainment processes. *Mon. Weather Rev.* **134**: 2318–2341.

Houghton DM. 1984. *Wind Strategy*. Fernhurst Books: Leamington Spa, UK.

Hu XM, Klein PM, Xue M. 2013. Evaluation of the updated YSU planetary boundary layer scheme within wrf for wind resource and air quality assessments. *J. Geophys. Res. Atmos.* **118**: 10490–10505.

Hunt JCR, Orr A, Rottman JW, Capon R. 2004. Coriolis effects in mesoscale flows with sharp changes in surface conditions. *Q. J. R. Meteorol. Soc.* **130**: 2703–2731.

James PM. 2007. An objective classification method for Hess and Brezowsky Grosswetterlagen over Europe. *Theor. Appl. Climatol.* **88**: 17–42.

Jenkinson AF, Collison P. 1977. *An Initial Climatology of Gales Over the North Sea*, Synoptic Climatology Branch Memorandom 62. Meteorological Office: Bracknell, UK.

Jones PD, Hulme M, Briffa KR. 1993. A comparison of Lamb circulation types with an objective classification scheme. *Int. J. Climatol.* **13**: 655–663.

Krogsaeter O, Reuder J, Hauge G. 2011. 'WRF and the marine planetary boundary layer'. In *Papers presented at the 12th Annual WRF Users' Workshop*. Boulder, CO. http://www.mmm.ucar.edu/wrf/users/workshops/WS2011/WorkshopPapers.php (accessed 8 November 2014).

Lyons WA. 1972. The climatology and prediction of the Chicago lake breeze. *J. Appl. Meteorol.* **11**: 1259–1270.

Mellor GL, Yamada T. 1982. Development of a turbulence closure model for geophysical fluid problems. *Rev. Geophys. Space Phys.* **20**: 851–875.

Miller STK, Keim BD, Talbot RW, Mao H. 2003. Sea breeze: Structure, forecasting and impacts. *Rev. Geophys.* **41**: 1011–1042.

Moore G, Renfrew I. 2005. Tip jets and barrier winds: A QUICKSCAT climatology of high speed wind events around Greenland. *J. Clim.* **18**: 3713–3725.

Nakanishi M. 2001. Improvement of the Mellor–Yamada turbulance closure model based on large-eddy simulation data. *Boundary-Layer Meteorol.* **99**: 349–378.

NCEP, NWS, NOAA, US Department of Commerce. 2000. 'NCEP FNL Operational Model Global Tropospheric Analyses, continuing from July 1999'. http:// rda.ucar.edu/datasets/ds083.2 (accessed 9 September 2014).

Pielke RA. 1991. Regional and mesoscale meteorological modeling as applied to air quality studies. *Air Pollut. Model. Appl. VIII* **32**: 259–289.

RenewableUK. 2014. 'Offshore energy'. http://www.renewableuk.com/en/renewable-energy/wind-energy/offshore-wind/index.cfm (accessed 8 November 2014).

Simpson JE. 1994. *Sea Breeze and Local Winds*. Cambridge University Press: Cambridge, UK.

Simpson JE, Mansfield DA, Milford JR. 1977. Inland penetration of sea-breeze fronts. *Q. J. R. Meteorol. Soc.* **103**: 47–76, doi: 10.1002/qj.49710343504.

Skamarock WC, Klemp JB. 2008. A time-split non-hydrostatic atmospheric model for weather research and forecasting applications. *J. Comput. Phys.* **227**: 3465–3485.

Steele CJ. 2013. 'Simulating sea-breeze type climatologies: Implications for wind energy, weather forecasting and sailing in the southern North Sea', PhD thesis. University of East Anglia: Norwich, UK.

Steele CJ, Dorling SR, von Glasow R, Bacon J. 2013. Idealized WRF model sensitivity simulations of sea breeze types and their effects on offshore windfields. *Atmos. Chem. Phys.* **13**: 443–461, doi: 10.5194/acp-13-443-2013.

Sterk HAM, Steeneveld GJ, Holtslag AAM. 2013. The role of snow-surface coupling, radiation, and turbulent mixing in modelling a stable boundary layer over Arctic sea ice. *J. Geophys. Res. Atmos.* **118**: 1199–1217, doi: 10.1002/jgrd.50158.

Sun WY, Ogura Y. 1980. Modeling the evolution of the convective planetary boundary layer. *J. Atmos. Sci.* **37**: 1558–1572.

Tijm ABC, van Delden AJ, Holtslag AAM. 1999. The inland penetration of sea breezes. *Contrib. Atmos. Phys.* **72**: 317–328.

Yerramilli A, Srinivas CV, Dasari HP, Tuluri F, White LD, Baham JM, Young JH, Hughes R, Patrick C, Hardy MG, Swanier SJ. 2009. Simulation of atmospheric dispersion of elevated releases from point sources in Mississippi Gulf coast with different meteorological data. *Int. J. Environ. Res. Public Health* **6**: 1055–1074, doi: 10.3390/ijerph6031055.

© 2014 The Authors. *Quarterly Journal of the Royal Meteorological Society* published by John Wiley & Sons Ltd on behalf of the Royal Meteorological Society.